J Nanopart Res (2017) 19:234
DOI 10.1007/s11051-017-3911-x

RESEARCH PAPER

PVP immobilized SiO_2 nanospheres for high-performance shear thickening fluid

Mei Liu · Qian Chen · Sheng Wang · Linfeng Bai · Min Sang · Wanquan Jiang · Shouhu Xuan · Xinglong Gong

Received: 9 March 2017 / Accepted: 30 May 2017

Abstract We develop a modified method to improve the rheological performance of SiO_2-based shear thickening fluid (STF). Directly adding surfactant into STF is the most common method to improve the rheological performance of SiO_2-based STF. However, the final viscosity increases quickly with the increase of shear rate, which is against for the practical applications. In this work, SiO_2 nanospheres are firstly modified by PVP K30 through an ethanol refluxing method and the modified SiO_2 nanospheres are used to prepare PVP@SiO_2-STF. Compared with the unmodified SiO_2 based STF (SiO_2-STF), the PVP@SiO_2-STF presents an obvious increase of shear thickening (ST) effects and the maximum viscosity increases by 7 times and the critical shear rates decrease about 10 times approximately. A reasonable explanation is proposed to interpret the influence of the modification methods on the rheological properties of STF. This work provides a new way to control the shear thickening behavior and also contributes to understand the mechanism of ST effect, which has an important significance to develop controllable STF.

Keywords Shear thickening fluid · Modified SiO_2 · PVP K30 · Rheological property · Dynamic behavior of nanostructures

Electronic supplementary material The online version of this article (doi:10.1007/s11051-017-3911-x) contains supplementary material, which is available to authorized users.

M. Liu · S. Wang · L. Bai · M. Sang · W. Jiang (✉)
Department of Chemistry, Collaborative Innovation Center of Suzhou Nano Science and Technology, University of Science and Technology of China (USTC), Hefei 230026, People's Republic of China
e-mail: jiangwq@ustc.edu.cn

Q. Chen · S. Xuan · X. Gong (✉)
CAS Key Laboratory of Mechanical Behavior and Design of Materials, Department of Modern Mechanics, USTC, Hefei 230027, People's Republic of China
e-mail: gongxl@ustc.edu.cn

Introduction

Shear thickening (ST) is a non-Newtonian flow behavior sometimes observed in concentrated suspensions of particles, exhibits a transition from fluid-like to solid-like state when subjected external sudden force. This behavior is reversible, meaning that the viscosity immediately decreases to initial state once the applied stress is relieved (Brown et al. 2010a, b; Brown and Jaeger 2014; Seto et al. 2013). Due to the unique features of STF, it sparks much curiosity to explore its origination and applications. In fact, people initially pay attention to this phenomenon due to its damage to industrial processes such as pipe jamming, mixing, and breakdown of spraying equipment. However, the rapid increase in viscosity of STF has been exploited in technological applications ranging from energy dissipation in soft body armors and speed limiters to spacecraft shielding concepts for mitigating highly energetic micrometeoroid/orbital debris impacts (Barnes 1989; Zhang et al. 2008; Kang et al. 2012; Lee et al. 2003; Cwalina 2016; Warren et al. 2013; Wagner and Wetzel 2007).

Published online: 28 June 2017

Although much progress has been made, the mechanism of shear thickening in dispersions is still in contention. Up to now, there are two generally accepted mechanisms accounting for shear thickening. One mechanism is an order-disorder transition (Hoffman 1972, 1974, 1982), in which a transition from ordered two-dimensional hexagonal packing layers of particles to a disordered array at some critical level of shear stress. This explanation is demonstrated by light diffraction and small angle neutron scattering experiments (Hoffman 1972, 1991; Chen et al. 1994). However, subsequent researchers claim that shear thickening in dispersions can occur without an order-disorder transition, which means that the order-disorder transition is not a required mechanism of shear thickening (Bender and Wagner 1996; Chow and Zukoski 1995). The second is hydrocluster mechanism (Brady and Bossis 1985), which claims that the particles tend to be pushed into together transiently by hydrodynamic lubrication forces above a critical shear rate and grow into large clusters, leading to a larger effective viscosity. This mechanism has been proved by the rheo-optical experiment (Bender and Wagner 1995), stress-jump rheological measurements (O'Brien and Mackay 2000), and neutron scattering (Laun et al. 1992; Newstein et al. 1999). Furthermore, combining fast confocal microscopy with simultaneous force measurements, Cheng et al. made it possible to directly observe clusters coinciding with the shear thickening regime. Stokesian dynamics simulations also supported this mechanism (Cheng et al. 2011; Bossis and Brady 1989; Boersma et al. 1992).

Besides the ST mechanism, the development of alternate method for controlling the shear thickening behavior is another challenge. Many empirical strategies ranging from altering particle surfaces and shape to modifying the solvent properties are developed (Ye et al. 2013; Egres and Wagner 2005). In pioneering work, various factors such as the characteristics of dispersed particles (including the maximum packing fraction, type, shape, size, polydispersion, surface chemistry property, and interparticle action), solvents, and additives are systematically studied (Yu et al. 2012; Maranzano and Wagner 2001; Qin et al. 2015; Sha et al. 2013; Brown et al. 2010a, b; Chang 2011; Shenoy and Wagner 2005; Xu et al. 2010; Liu et al. 2016). Among these factors, additives play an important role in tuning the rheological properties of STF. Due to the limited varieties of STF, the rheological properties are relatively unaltered, which greatly reduces the potential scope of practical application. Different kinds of additives can be used to modify the dispersed particle, tune the fluidity of the solvents, and adjust the interaction between the particle and the solvent, and thus regulating the rheological properties and expanding the potential use of STF. Many efforts have been done to study the influences of additives on the rheological properties of the dense suspensions. Frank et al. introduce acid (HCl, HNO_3), base (KOH, NaOH), and (KNO_3) to change the interparticle forces to tune the ST behavior of oxide dispersions (Franks et al. 2000). Yang et al. study the effects of pH on rheological behaviors of titanium dioxide suspensions by altering particle surface charge via adding HNO_3 or NaOH (Yang et al. 2001). Ye et al. study the influence of surfactant kinds on ST behavior in concentrated dispersions and discuss the enhancement mechanism of ST effects in STF (Ye et al. 2013). Above all, a series of work have been done in terms of the effects of the kind, concentration, molecular weight of additives to rheological behavior of dense dispersions.

However, the influence of the different modification methods on the rheological behavior of dense dispersion has been rarely investigated. The most commonly usage of additives is added into the dispersion directly (Ye et al. 2013). Even the same additive, the different added methods also lead to different influence on the rheological behavior of the dispersion. For example, the dispersed particles are modified first and adding the same additive in to the dispersion directly; the main object modified by the former method is the dispersed particles while the latter mainly changes the solvent properties of the dispersion. So, it is necessary to study the influence of different modification methods on the rheological properties of dense dispersions to reveal the mechanism of the fluid variation caused by the additive, which has important significance in developing controllable STF and contributes to further understand the mechanism of ST.

Polyvinyl pyrrolidone $(C_6H_9NO)_n$ is a nonionic and water soluble macromolecular compound, which has the general properties of colloid protection, emulsification, dispersancy, cohesiveness, solubilization, coacervation. It has been widely investigated and applied in industry, medicine, and food production (Komal et al. 2011; El-Badry and Fathy 2006; Swei and Talbot 2003; Namekawa et al. 2011; Parmar et al. 2011). In this work, PVP K30 is used as the additive to study the influence of different

modification methods on the rheological properties of STF. A possible explanation is proposed to interpret the reason of the different influence on the rheological performance caused by the two different modification methods via hydrocluster mechanism. At the same time, a modified method is developed to enhance the rheological performance of STF, which is significant to open a new way to control the ST behavior and help to study the mechanism of ST.

Experimental methods

Materials

Tetraethylorthosilicate (TEOS, liquid, chemical pure), ethanol (liquid, analytical reagent), ammonium hydroxide ($NH_3 \cdot H_2O$, liquid, 25–28%, analytical reagent), and poly (ethylene glycol) 200 (PEG 200, liquid, analytical reagent) are all purchased from Sinopharm Chemical Reagent Co. Polyvinyl pyrrolidone (PVP K30, solid) is purchased from Aladdin. All chemicals are used directly as received without further treatment. Re-distilled water is used in this work (the resistivity is ~18 MΩ cm).

The preparation of STFs

Firstly, monodisperse SiO_2 nanospheres are synthesized via the modified Stöber sol-gel method (Stöber et al. 1968; Bogush et al. 1988; Farmany et al. 2016).

SiO_2-STF is prepared by adding a certain amount of SiO_2 nanospheres into PEG200, and the mixture is mixed in a ball crusher for 24 h. The obtained SiO_2-STF is sealed in a vial before use (Liu et al. 2016).

The PVP immobilized SiO_2 is prepared as follows. SiO_2 nanospheres of 3.5 g are dispersed in 100 mL ethanol by ultrasonic process for 30 min and then adding extra 50 mL ethanol to the solution to guarantee SiO_2 nanospheres dissolving thoroughly. SiO_2 nanosphere dispersion of 150 mL is added into 250-mL three-necked, round-bottomed flask fitted with a mechanical stirrer. A certain amount of PVP K30 is mixed with the 150-mL SiO_2 nanosphere solution through mechanical stirring and the mixed solution is refluxed with ethanol throughout the experiment for 12 h at 85 °C in a water bath. The percentages of PVP K30 are controlled as 1.0% (0.035 g), 2.0% (0.070 g), 3.0% (0.105 g), 4.0% (0.140 g), 5.0% (0.175 g), 6.0% (0.210 g), and 7.0% (0.245 g) of the mass of SiO_2 nanospheres (3.5 g). The product of PVP K30 immobilized SiO_2 nanospheres (PVP@SiO_2) is obtained through centrifugation and washed two times by ethanol. The final product is dried in the vacuum oven at 50 °C. The dried PVP@SiO_2 is grinded in the ball crusher.

Then, adding a certain amount of PVP@SiO_2 into PEG 200 and the mixture is mixed in a ball crusher to obtain a homogeneous dispersion. The process of ball mill lasts about 24 h, and the final product is collected when no large-scale aggregation is found in the suspension. The final obtained suspension is PVP@SiO_2-STF and is sealed in a vial before use.

PVP-SiO_2-STF is prepared as follows. A certain amount of pristine SiO_2 nanospheres and PVP K30 are added into PEG 200 directly. The percentages of PVP K30 are controlled as 0.2% (0.006 g), 0.4% (0.012 g), 0.6% (0.018 g), 0.8% (0.024 g), 1.0% (0.030 g), and 1.2% (0.036 g) of the mass of SiO_2 nanospheres (3 g). The mixture is mixed in a ball crusher to obtain a homogeneous dispersion. The final obtained PVP-SiO_2-STF is sealed in a vial before use.

Rheological measurements

The rheological properties of the STF are measured by using the rheometer (Physical, MCR301, Anton Paar) at 25 °C with cone-plate having a cone angle of 2° and a diameter of 25 mm. The rheological properties of each sample are measured under static loading conditions. The steady-shear tests are conducted with a gap size of 0.05 mm. In order to remove loading effects, a pre-shear of 1 s^{-1} is applied for 20 s before collecting the experimental data.

Characterization

The particle size and macroscopic features are determined by a field emission scanning electron microscope (20 kV, JEOL JSM-6700F SEM). The thickness of the shell is observed by a transmission electron microscopy (TEM, JEM-2011, Japan) with an accelerating voltage of 200 kV. Infrared (IR) spectra are measured by a Nicolet Model 759 Fourier transform infrared (FT-IR) spectrometer in the wavenumber range 4000–500 cm^{-1} with using a KBr wafer. X-ray photoelectron spectra (XPS) are measured on an ESCALAB 250. Thermogravimetric (TG) analysis is performed in air from room temperature to 700 °C at the rate of 10 °C/min on a DTG-60H thermogravimetric instrument.

Results and discussion

Preparation and characterization of the PVP@SiO_2

In this experiment, SiO_2 nanospheres are prepared by modified Stöber sol-gel method. Figure 1 shows SEM (a–c), TEM (d–f) images of the SiO_2 nanospheres and energy dispersive spectrometer (EDS) mapping spectra (g–l) of each element on the surface of the PVP@SiO_2. From SEM (a–c) and TEM (d–f) images, we can clearly observe that the SiO_2 nanospheres are monodisperse and the diameter mainly concentrated in 310 nm. In order to confirm the successful modification of PVP K30 molecules on the surface of SiO_2 nanospheres, the energy dispersive spectrometer (EDS) mapping spectra of the elements existed on the surface of PVP@SiO_2 is conducted. Energy dispersive spectrometer (EDS) mapping spectra of each element (nitrogen (i), carbon (j), silicon (k), and oxygen (l)) on the surface of the PVP@SiO_2 (g, the modification concentration of PVP K30 is 6%) indicates the existence of nitrogen and carbon that mainly comes from the PVP K30 modified on the surface of SiO_2 nanospheres, which further shows that PVP K30 successfully modifies the SiO_2 nanospheres through ethanol reflux method.

The FTIR spectra (Fig. 2) of SiO_2 nanospheres (a), PVP@SiO_2 (the concentration of PVP K30 are 1.0% (b), 4.0% (c), and 7.0% (d)) and pure PVP K30 (e) are investigated. Figure 2a shows the typical FTIR spectra of PVP@SiO_2. The signal at 1000^{-1}–1100 cm^{-1} is attributed to the Si–O–Si bond asymmetric stretching vibration. The peaks around 3432 cm^{-1} are ascribed to the stretching vibrations of the oxygen-hydrogen (–OH) bonds. The spectra of PVP K30 (Fig. 2e) shows characteristic peaks at 2954 cm^{-1} (C–H stretch) and 1675 cm^{-1} (C═O stretch). The peaks of Fig. 2b, c, d have a slightly red shift compared with the peaks of SiO_2 (Fig. 2a) because of the modification by PVP K30.

XPS spectra (Fig. 3) are employed to analyze the surface of the pristine SiO_2 nanospheres and PVP@SiO_2. Strong O1s and Si2p peaks are clearly found in the spectra of the SiO_2 nanospheres (Fig. 3a). A tiny C1s peak is present in the spectra, which may be due to the residual ethanol or $–OCH_2CH_3$ groups on the surface of the SiO_2 nanospheres. A distinctive nitrogen signal can be clearly observed and the intensity of the C1s peaks is also obviously enhanced in Fig. 3b. The detective depth of the XPS is about 10 nm and the surface of modification is thinner; thus, a Si2p signal is also present in the PVP@SiO_2. These results demonstrate the successful modification of PVP K30 on SiO_2 nanospheres because the N1s and C1s signals in the XPS spectra mainly arise from the PVP K30, which contains large number of pyrrolidone components.

In order to further study the effects of the PVP K30 on the surface of SiO_2 nanospheres, the thermogravimetric analysis is performed. Figure 4 is the thermogravimetric curve of the pristine SiO_2 nanospheres (red line) and the PVP@SiO_2 (the modification concentrations of PVP K30 are 2.0% (green line), 4.0% (the orange line), and 6.0% (blue line)). The weight loss from 0 to 100 °C is attributed to the adsorbed water. With further increasing the temperature to 500 °C, the residue organic groups in the SiO_2 nanospheres collapse. The total weight losses of SiO_2 nanospheres and PVP@SiO_2 (the modification concentrations of PVP K30 are 2.0% (green line), 4.0% (the orange line), and 6.0% (blue line)) are 10.4, 10.8, 11.61, and 12.2%, respectively. For the PVP@SiO_2, the total weight losses are attributed to the decomposition of the PVP K30 and increase with the increasing of the modification concentration of PVP K30, which indicates that the existence of PVP K30 on the surface of SiO_2 nanospheres increases when the modification concentration of PVP K30 increases.

The rheological behavior of the PVP@SiO_2-STF

Figure 5a shows the photos of PVP@SiO_2 based STF sealed in vial. From the photos, we can observe that when the vial is turned over, the STF flows immediately and restores to its initial state quickly when the vial is put down motionless, which indicates the good fluidity. Figure 5b shows a representative rheological curve of the viscosity versus shear rate for PVP@SiO_2 based STF. The insets are the pictures taken at three critical conditions during a steady-shear experiment. A slightly shear thinning behavior is observed initially when the shear rate is below 10 s^{-1}, in which the viscosity decreases with increasing shear rate. However, the viscosity increases dramatically (shear thickening) when the shear rate is higher than 10 s^{-1}. The characteristic of dramatic increase in viscosity when the shear rate reaches to the critical shear rate distinguishes STF from other suspensions. The increase of viscosity leads the STF transforming from fluid state to solid state, which can be observed through the surface changes of STF. The inset photos of the STF surface are taken at three

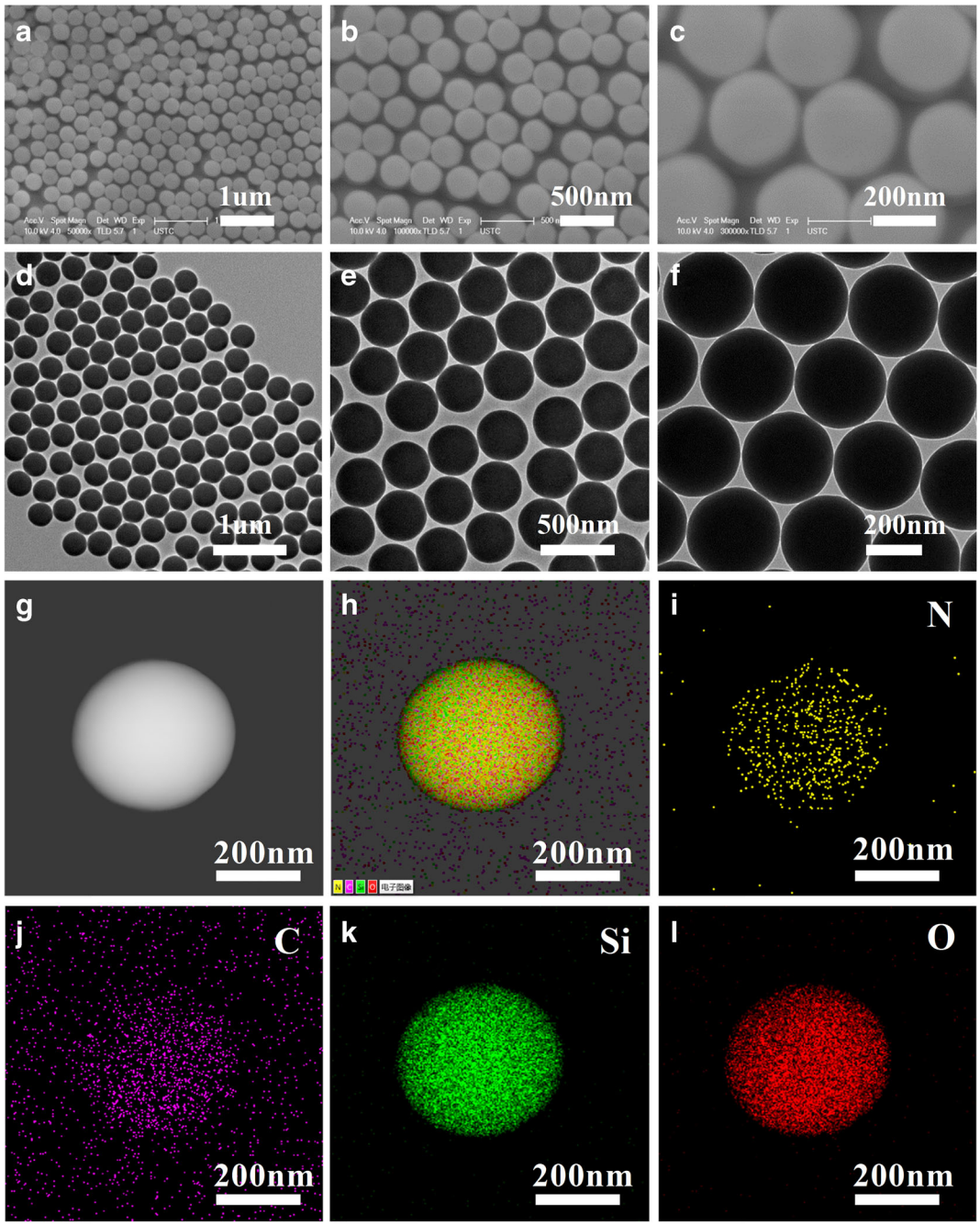

Fig. 1 SEM (**a**–**c**) and TEM (**d**–**f**) images of the SiO_2 nanospheres. Energy dispersive spectrometer (EDS) mapping spectra (h) of elements including nitrogen, carbon, silicon, and oxygen on the surface of PVP@SiO_2. Energy dispersive spectrometer (EDS) mapping spectra of each element (nitrogen (**i**), carbon (**j**), silicon (**k**), oxygen (**l**)) on the surface of PVP@SiO_2 (**g** the modification concentration of PVP K30 is 6%)

critical conditions during a steady-shear experiment (from left to right), (i) the initial state, (ii) near the critical shear rate, and (iii) shear thickening state (the arrows correspond to data points). The surface state has no obvious visible change at the critical shear rate compared with the initial state. However, instabilities formed in shear thickening region lead part of the sample to be ejected, which cause the viscosity decreasing even the

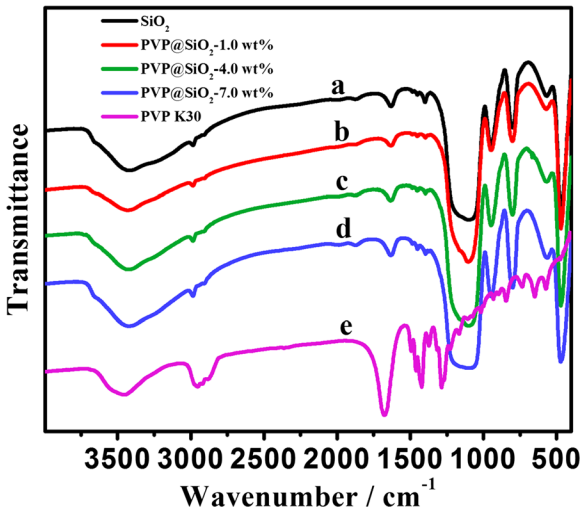

Fig. 2 FTIR spectra of SiO_2 nanospheres (**a**), PVP@SiO_2 (the concentration of PVP K30 are 1.0% (**b**), 4.0% (**c**), and 7.0% (**d**)) and pure PVP K30 (**e**)

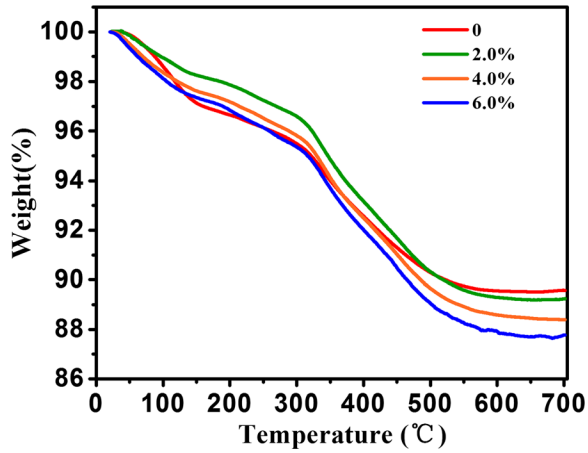

Fig. 4 TG of the pristine SiO_2 nanospheres (*red line*) and the PVP@SiO_2 (the modification concentrations of PVP K30 are 2.0% (*green line*), 4.0% (the *orange line*), and 6.0% (*blue line*))

shear rate keeps increasing and it not represents the true STF viscosity. The transition from fluid state to solid state is thought to be related to the formation of hydroclusters in STF. Additionally, Fig. 5b shows the curve of critical shear rate and associated shear stress and the point at which the slope changes suddenly marks the onset of shear thickening behavior.

Figure 6a shows the static rheological properties of PVP@SiO_2-STF with different PVP K30 concentrations (1.0% (0.035 g), 2.0% (0.07 g), 3.0% (0.105 g),

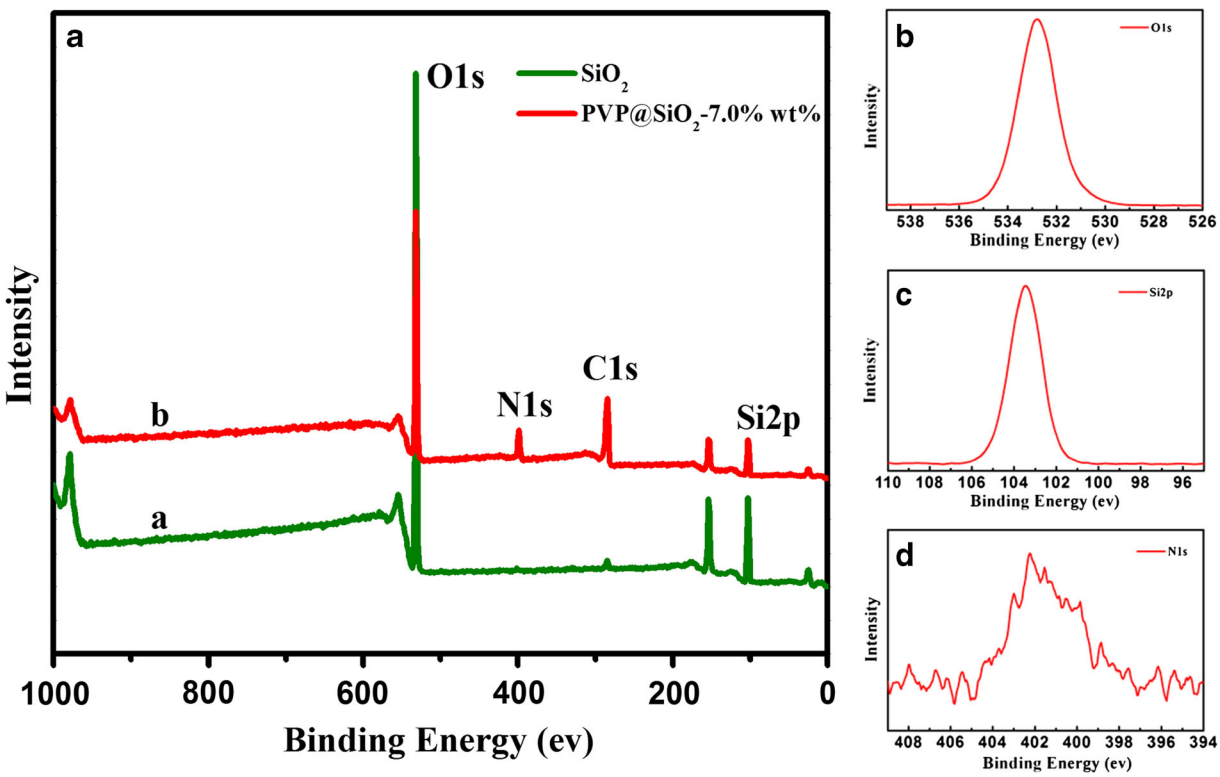

Fig. 3 Broad-range XPS spectra (**a**) of SiO_2 nanospheres (*a*) and PVP@SiO_2 (*b*, the concentration of PVP K30 is 7%). The high resolution spectra for oxygen (**b**), silicon (**c**), and nitrogen (**d**) of broad-range XPS spectra (**a**) of PVP@SiO_2 (*b*)

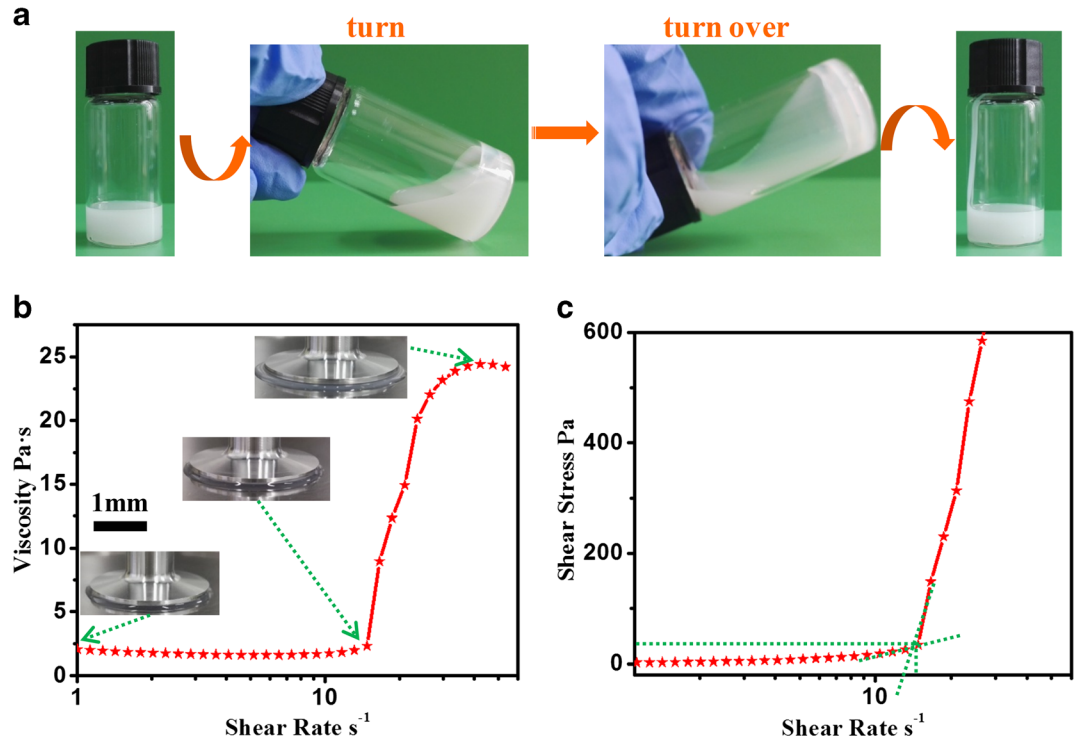

Fig. 5 The pictures (**a**) show the good fluidity of PVP@SiO_2-STF. Viscosity versus shear rate for PVP@SiO_2 based STF with the mass fraction of 67% (**b**). The insets (**b**) are the pictures taken at three critical conditions during a steady-shear experiment. The determination of the critical shear rate and associated shear stress based on the sudden change in the slope of the shear stress versus shear rate curve (**c**)

4.0% (0.105 g), 5.0% (0.175 g), 6.0% (0.21 g), and 7.0% (0.245 g)). Figure 6b–d is the analysis of the critical factors of the curve in Fig. 6a. The variation trends of the critical shear rate, the initial viscosity, and the maximum viscosity with different PVP K30 concentrations of Fig. 6a are analyzed in Fig. 6b–d. Figure 6b shows that the critical shear rate is 221.1 s^{-1} of the SiO_2-STF (without being modified with PVP K30) when the volume fraction of the SiO_2 nanospheres in the suspension is 54.6%. However, the critical shear rates of PVP@SiO_2-STF decrease abruptly at the same volume fraction. They are 33.1, 20.8, 14.1, 13.4, 16.9, 20.18, and 26.0 s^{-1} when the corresponding percentages of PVP K30 are 1.0, 2.0, 3.0, 4.0, 5.0, 6.0, and 7.0%. The critical shear rates decrease about 10 times after the SiO_2 nanospheres are modified with PVP K30. The initial viscosity of the SiO_2 nanospheres (without being modified with PVP K30) based STF is 1.2 Pa·s. The initial viscosities of PVP@SiO_2-STF are 1.6, 1.8, 2.13, 2.1, 2.0, 2.1, and 2.0 Pa·s corresponding to the series of percentages of PVP K30. This indicates that there is little influence on the initial viscosity of suspensions after the SiO_2 nanospheres are modified with PVP K30. The maximum viscosity of the SiO_2-STF is 3.6 Pa·s. The maximum viscosities of PVP@SiO_2-STF are 10.76, 15.11, 16.33, 24.2, 20.42, 18.04, and 15.2 Pa·s corresponding to different percentages of PVP K30. Obviously, when the percentage of PVP K30 is 4.0%, the final PVP@SiO_2-STF exhibits an optimal ST effect.

Therefore, the rheological properties of STF are changed dramatically after the SiO_2 nanospheres are modified with PVP K30. The critical shear rate decreases and the maximum viscosity increases obviously. When the percentage of PVP K30 is 4.0%, the maximum viscosity reaches up to the optimal value. There is little influence on the initial viscosity of STF. The modification of SiO_2 nanospheres with PVP K30 greatly enhanced the degree of shear thickening of STF compared with pristine SiO_2 nanospheres.

Here, besides the immobilization method, the STF which is prepared by directly doping PVP surfactant is also investigated. Figure 7a shows the static rheological properties of PVP doped SiO_2-STF, in which the

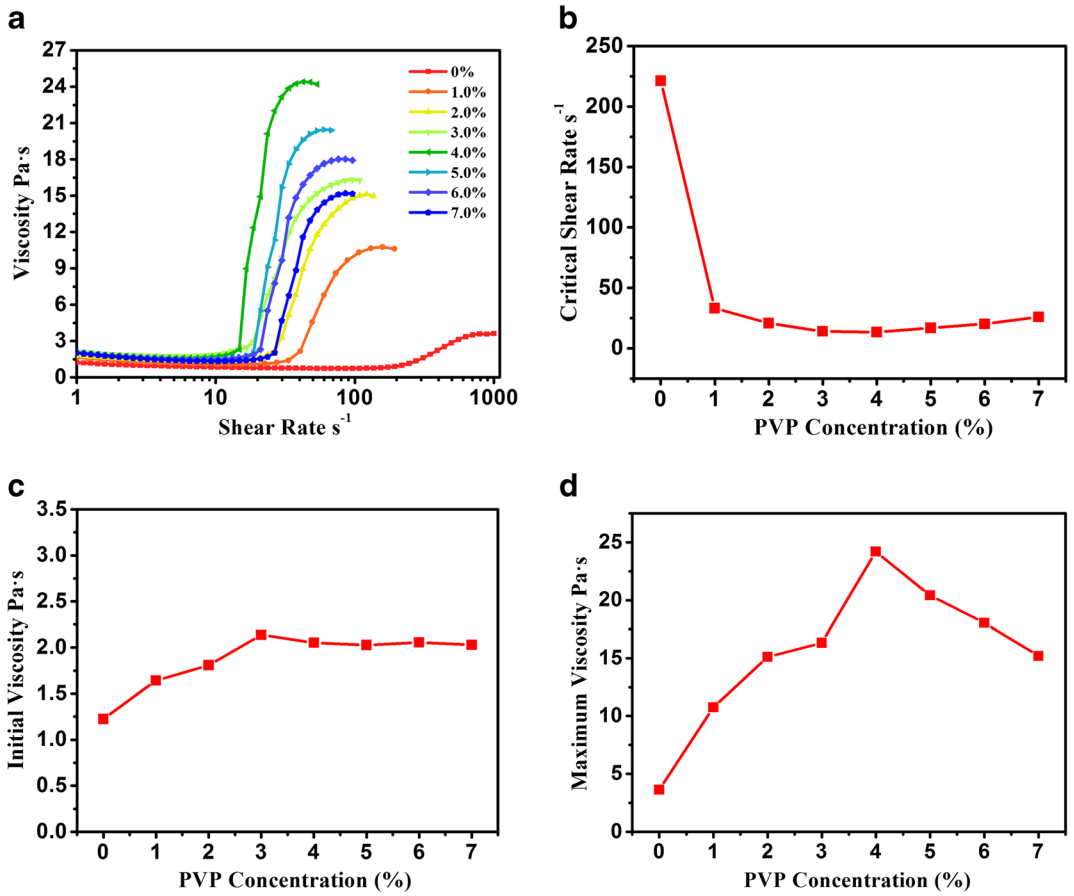

Fig. 6 Viscosity versus shear rate for PVP@SiO_2-STF (**a**). The variation trends of the critical shear rate (**b**), the initial viscosity (**c**), and the maximum viscosity (**d**) under different PVP K30 concentrations (%) of figure **a** (the volume fraction is 54.6%)

percentages of PVP K30 vary from 0 to 0.2, 0.4, 0.6, 0.8, 1.0, and 1.2%. Figure 7b–d is the critical factors of rheological properties concluding the critical shear rate, the initial viscosity, and the maximum viscosity of the PVP doped SiO_2-STF. Figure 7b shows that the critical shear rate is 221.1 s^{-1} of the SiO_2-STF when the volume fraction of the SiO_2 nanospheres in the suspension is 54.6%. After mixing with PVP K30, the critical shear rates of PVP-SiO_2-STF decrease abruptly. They are 42.1, 21.1, 9.1, 1.8, 1.4, and 33.87 s^{-1} when the corresponding percentages of PVP K30 are 0.2, 0.4, 0.6, 0.8, 1, and 1.2%.The initial viscosities are 1.4, 1.2, 1.5, 1.6, 2.5, and 2.9 Pa·s when the corresponding percentages of PVP K30 are 0.2, 0.4, 0.6, 0.8, and 1% (Fig. 7c). The initial viscosity increases slightly with the increasing of the PVP K30 percentage. However, the initial viscosity increases to 32.95 Pa·s suddenly when the percentage of PVP K30 reaches to 1.2%. The maximum viscosities are 3.6, 8.7, 12.9, 16.7, 27.4, 20.69, and 28.1 Pa·s corresponding to the series of percentages of PVP K30. Clearly, 0.6% is the optimal value of the PVP K30 percentage added to the PVP-SiO_2-STF.

Based on the above result, it is found that the PVP doping influences the rheological properties of the SiO_2-STF. Firstly, it decreases the critical shear rate and increases the maximum viscosity with the increasing of the concentration of PVP K30. There is an optimal value of the concentration of PVP K30. The initial viscosity of STF will become too large and decrease the shear thickening when the concentration of PVP K30 reaches to a certain value. Additionally, the viscosity increases quickly with the increasing of the shear rate, which is a disadvantage in practical applications.

In order to study the influence of the PVP K30 modified of SiO_2 nanospheres on the rheological properties of STF, the rheological properties of SiO_2-STF with a series of volume fractions are also compared with PVP@SiO_2-STF (Fig. 8). When the volume fractions of

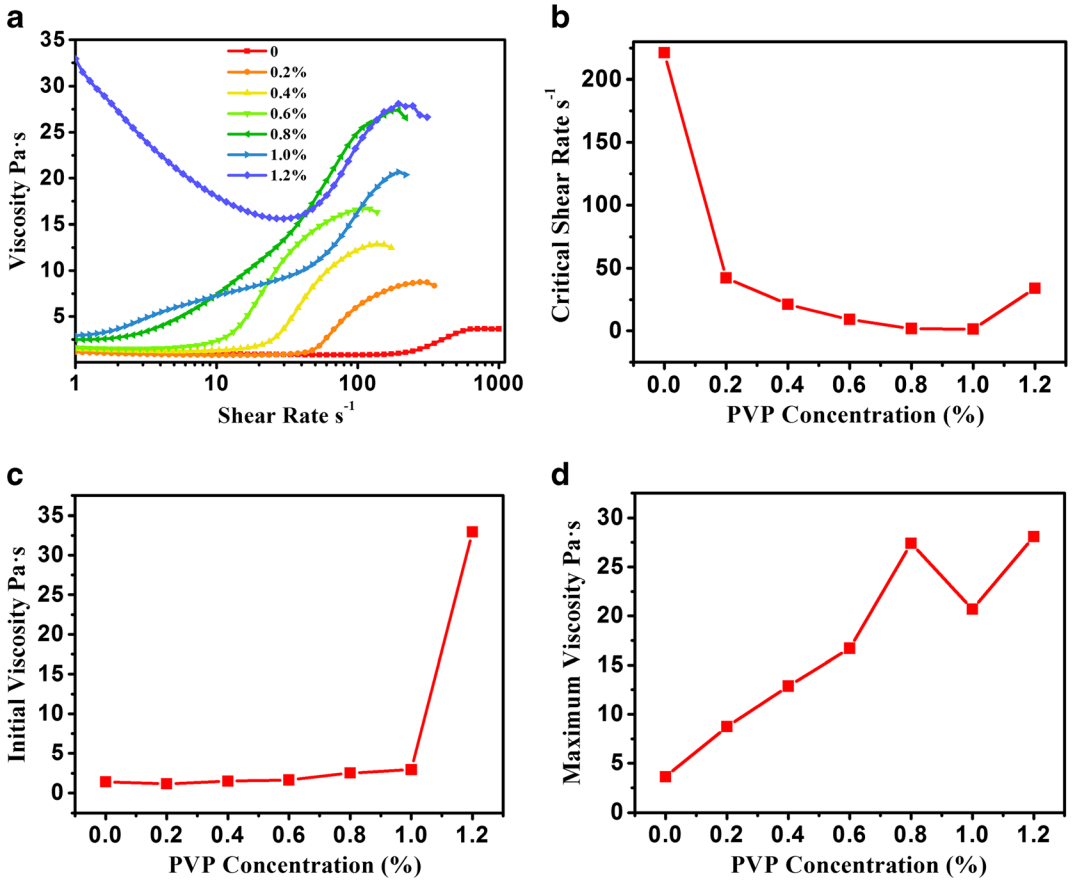

Fig. 7 Viscosity versus shear rate for PVP-SiO_2-STF (**a**). The variation trends of the critical shear rate (**b**), the initial viscosity (**c**), and the maximum viscosity (**d**) under different PVP K30 concentrations (%) in figure **a** (the volume fraction is 54.6%)

SiO_2-STFs are 54.6, 55.7, 56.8, and 58.0%, the critical shear rates are 225.2, 172.9, 122.2, and 114.0 s^{-1}, the initial viscosities are 1.2, 1.5, 2.5, and 2.3 Pa·s, and the maximum viscosities are 3.6, 5.6, 14.3, and 21.4 Pa·s, respectively. Compared with the static rheological properties of SiO_2-STF, when the volume fraction of PVP@SiO_2-STF (the percentage of PVP K30 is 4%) is 54.6%, the critical shear rates are 15.0 s^{-1}, the initial viscosity is 2.0 Pa·s, and the maximum viscosity is 24.1 Pa·s, respectively. As a result, increasing the mass fraction of SiO_2-STF can decrease the critical shear rate and enhance the degree of shear thickening to a certain extent. However, the improvement is slow and less obvious. After the SiO_2 nanospheres are modified with PVP K30, the critical shear rate decreases to 15 times and the maximum viscosity increases about 7 times at the same volume fraction (54.6%). The maximum viscosity is almost identical with the SiO_2-STF at the volume fraction of 58%. As a result, the modification

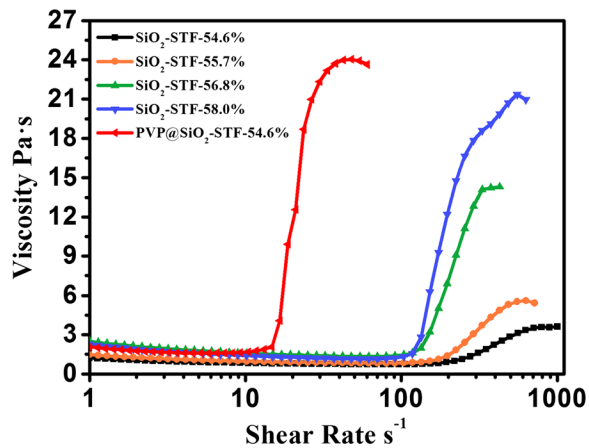

Fig. 8 Viscosity versus shear rate for SiO_2-STF (the volume fractions of SiO_2 nanospheres are 54.6, 55.7, 56.8, and 58.0%) and PVP@SiO_2-STF (the volume fraction is 54.6% and the percentage of PVP K30 is 4%)

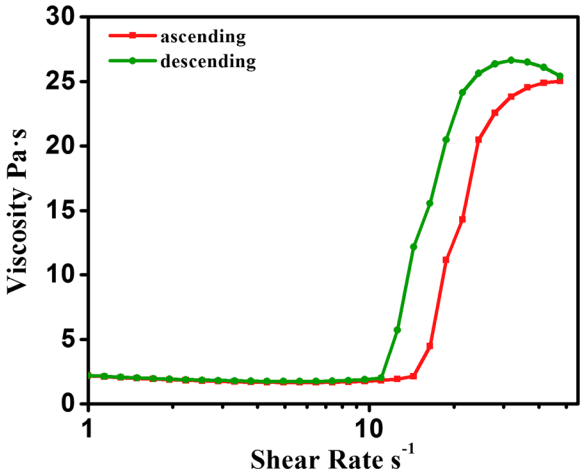

Fig. 9 Reversible shear thickening behavior of the PVP@SiO_2-STF with the volume fraction of 54.6% (the percentage of PVP K30 is 4%)

of SiO_2 nanospheres with PVP K30 enhances the shear thickening effect, which has an important significance in wearable soft armor and spacecraft shielding.

In this work, the reproducibility of PVP@SiO_2-STF is further studied. Reproducibility is one of the most important properties of STF in practical applications. Figure 9 shows the viscosity of the PVP@SiO_2-STF (the percentage of PVP K30 is 4%) with the volume fraction of 54.6% measured for both ascending and descending shear rate sweeps. There is a slight decrease in viscosity at a low shear rate, while it increases quickly as soon as the shear rate reaches the critical shear rate. At the same time, the viscosity first slightly increases and then decreases immediately when the shear rate decreases. It should be noted that the viscosity measurements are in good agreement at the same shear rate, which indicates that the shear thickening behavior of the PVP@SiO_2-STF is reversible. The hydroclusters formed in the shear thickening period can decompose and disperse in the dispersed phase again as soon as hydrodynamic lubrication is decreased. Therefore, the ST effect of PVP@SiO_2-STF has excellent cyclic reversibility.

The mechanism of the interaction between SiO_2 nanospheres in the STF with different methods of modification

Scheme 1 is the illustrated of the mechanism of the interaction between SiO_2 nanospheres in PVP@SiO_2-STF (Scheme 1a) and PVP-SiO_2-STF (Scheme 1b). As we know, PVP K30 is a kind of nonionic surfactant that contained polar and nonpolar groups; it can be adsorbed on the surface of SiO_2 nanospheres through physical-chemical effect, such as physical absorption and hydrogen bonding. In the immobilization method, due to the fact that SiO_2 nanospheres are firstly modified with PVP K30 via ethanol reflux, the PVP K30 is mainly located on the surface of SiO_2 nanospheres (the illustration is showed in Scheme 1a). In the second method, PVP K30

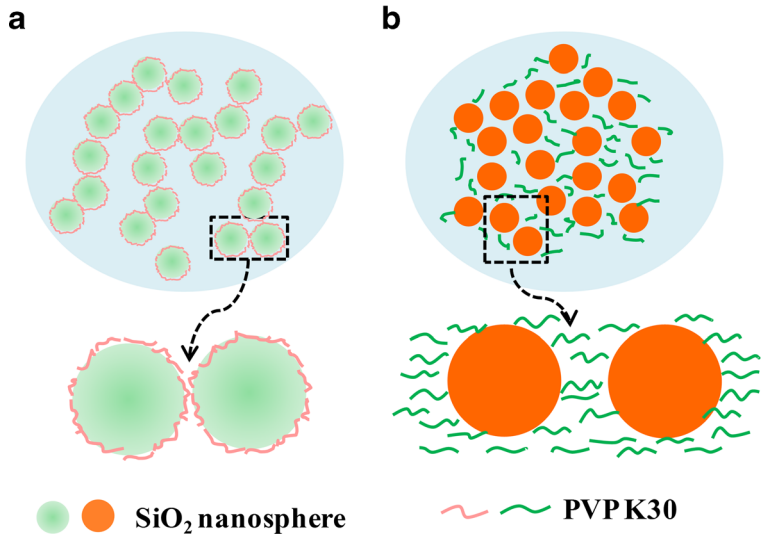

Scheme 1 The illustrations of the mechanism of the interaction between SiO_2 nanospheres in the STF (PVP@SiO_2-STF (**a**), PVP-SiO_2-STF (**b**)) with different modification methods

is added to the SiO_2-STF and dispersed uniformly through ball milling. Most of the PVP K30 exists in dispersing medium. Of course, there is also a small amount of PVP K30 adsorbing on the surface of SiO_2 nanospheres (Scheme 1b illustrates the state of the distribution of SiO_2 nanospheres in STF).

According to the hydrocluster mechanism, shear thickening arises from particle clustering induced by short-ranged hydrodynamic lubrication forces (Cheng et al. 2011). The interaction forces between particles play a critical role in the rheology of the dense suspension. Compared with SiO_2 nanospheres, the existence of PVP K30 on the surface of SiO_2 nanospheres improves the dissolving capacity and the stability of the dispersion due to the enhancement of the interaction force between the particle and the solvent. It is reported that repulsive interaction led to higher critical shear rate, while lubrication hydrodynamic interaction produced lower critical shear rate and severe ST (Kalman and Wagner 2009; Franks et al. 2000). The molecular chains on the surface improve the lubrication hydrodynamic interaction between particles, which leads to lower critical shear rate and severe ST. This agrees well with our experiment results. However, this phenomenon does not indicate that the more PVP K30 on the surface of SiO_2 nanospheres, the more severe of the ST effect. When the amount of PVP K30 is too much, the interaction forces between particles and the solvent are too strong due to large amounts of PVP K30 chains that existed on the surface of SiO_2 nanospheres. This will impede the movement of particles and suppress the rapid formation of hydroclusters when the suspension subjected high shear rate, which will then destroy the shear thickening. So, there is an optimum value for the PVP K30 and the optimal modification concentration is 4% in this experiment (Fig. 6).

In the second kind of STF (PVP@SiO_2-STF), the PVP K30 is well dispersed in suspension through ball milling. Due to the improvement of lubrication between particles, the critical shear rate is decreased. However, due to the molecule chains of PVP K30 existed in the solvent, it will also hinder the fast movement of particles. Therefore, the viscosity increases quickly with the increasing of shear rate, which reduces the liquidity of the STF and it is not beneficial to the practical application that desires the good flexibility under small disturbance. There is an optimum value of the PVP K30 concentration and the value is 0.6% in this experiment. Above the optimum value, the initial viscosity increases dramatically due to large amounts of molecule chains exist in suspension that hinders the free movement of particles, which also agrees with the experiment results (Fig. 7).

Based on above analysis, it can be concluded that the two methods have different influence on the rheological properties of STF. The PVP@SiO_2-STF is composed with SiO_2 nanospheres modified by PVP K30 via ethanol reflux first exhibits a great improvement of the degree of shear thickening, which is an excellent modification method to improve the rheological properties of STF. In PVP-SiO_2-STF, PVP K30 is directly added to the mixture of SiO_2 nanospheres and PEG 200 through ball milling. The degree of shear thickening is enhanced to some extent. However, the viscosity increased quickly with the increasing of shear rate, which limits its practical application.

Conclusion

In this work, an alternate method is developed to improve the rheological performance of STF. SiO_2 nanospheres are modified by PVP K30 via ethanol reflux for 12 h firstly and the PVP immobilized SiO_2 nanospheres are used to prepare STF. Compared with traditional method, the present method that modifies SiO_2 nanospheres firstly enhances the rheological properties of SiO_2-STF dramatically. The critical shear rate decreases about 16 times and the maximum viscosity increases about 7 times. Shear thickening effect increases obviously. A reasonable explanation is proposed to interpret the different influence of the two methods on the shear thickening behavior through hydrocluster mechanism. It is the first time to use this modified method to improve the rheological properties of STF, which provides a new way to tuning the ST behavior and contributes to better understand the mechanism of ST.

Acknowledgements Financial supports from the National Natural Science Foundation of China (Grant Nos. 11372301). The Fundamental Research Funds for the Central Universities (WK2480000002) and the Strategic Priority Research Program of the Chinese Academy of Sciences (Grant No. XDB22040502)

are gratefully acknowledged. This work was also supported by Collaborative Innovation Center of Suzhou Nano Science and Technology.

Compliance with ethical standards

Conflict of interest The authors declare that they have no conflict of interest.

References

Barnes HA (1989) Shear-thickening ("Dilatancy") in suspensions of nonaggregating solid particles dispersed in Newtonian liquids. J Rheol 33:329–366

Bender JW, Wagner NJ (1995) Optical measurement of the contributions of colloidal forces to the rheology of concentrated suspensions. J Colloid Interface Sci 172:171–184

Bender J, Wagner NJ (1996) Reversible shear thickening in monodisperse and bidisperse colloidal dispersions. J Rheol 40:899–916

Boersma WH, Laven J, Stein HN (1992) Viscoelastic properties of concentrated shear-thickening dispersions. J Colloid Interface Sci 149:10–22

Bogush GH, Tracy MA, Zukoski CF (1988) Preparation of monodisperse silica particles: control of size and mass fraction. J Non-Cryst Solids 104:95–106

Bossis G, Brady JF (1989) The rheology of Brownian suspensions. J Chem Phys 91:1866–1874

Brady JF, Bossis G (1985) The rheology of concentrated suspensions of spheres in simple shear flow by numerical simulation. J Fluid Mech 155:105–129

Brown E, Jaeger HM (2014) Shear thickening in concentrated suspensions: phenomenology, mechanisms and relations to jamming. Rep Prog Phys 77:046602

Brown E, Forman NA, Orellana CS, Zhang H, Maynor BW, Betts DE, De Simone JM, Jaeger HM (2010a) Generality of shear thickening in dense suspensions. Nat Mater 9:220–224

Brown E, Zhang HJ, Forman NA, Maynor BW, Betts DE, DeSimone JM, Jaeger HM (2010b) Shear thickening in densely packed suspensions of spheres and rods confined to few layers. J Rheol 54:1023–1046

Chang L (2011) Shear-thickening behaviour of concentrated polymer dispersions under steady and oscillatory shear. J Mater Sci 46:339–346

Chen LB, Chow MK, Ackerson BJ, Zukoski CF (1994) Rheological and microstructural transitions in colloidal crystals. Langmuir 10:2817–2829

Cheng X, McCoy JH, Israelachvili JN, Cohen I (2011) Imaging the microscopic structure of shear thinning and thickening colloidal suspensions. Science 333:1276–1279

Chow MK, Zukoski CF (1995) Nonequilibrium behavior of dense suspensions of uniform particles: volume fraction and size dependence of rheology and microstructure. J Rheol 39:33–59

Cwalina CD (2016) Shear thickening fluids for enhanced protection from micrometeoroids and orbital debris. University of Delaware, Newark

Egres RG, Wagner NJ (2005) The rheology and microstructure of acicular precipitated calcium carbonate colloidal suspensions through the shear thickening transition. J Rheol 49:719–746

El-Badry M, Fathy M (2006) Enhancement of the dissolution and permeation rates of meloxicam by formation of its freeze-dried solid dispersions in Polyvinylpyrrolidone K-30. Drug Dev Ind Pharm 32:141–150

Farmany A, Mortazavi SS, Mahdavi H (2016) Ultrasond-assisted synthesis of Fe_3O_4/SiO_2 core/shell with enhanced adsorption capacity for diazinon removal. J Magn Magn Mater 416:75–80

Franks GV, Zhou ZW, Duin NJ, Boger DV (2000) Effect of interparticle forces on shear thickening of oxide suspensions. J Rheol 44:759–779

Hoffman RL (1972) Discontinuous and dilatant viscosity behavior in concentrated suspensions. I. Observation of a flow instability. Trans Soc Rheol 16:155–173

Hoffman RL (1974) Discontinuous and dilatant viscosity behavior in concentrated suspensions. II. Theory and experimental tests. J Colloid Interface Sci 46:491–506

Hoffman RL (1982) Discontinuous and dilatant viscosity behavior in concentrated suspensions III. Necessary conditions for their occurrence in viscometric flows. Adv Colloid Interf Sci 17:161–184

Hoffman RL (1991) Interrelationships of particle structure and flow in concentrated suspensions. MRS Bull 16:32–37

Kalman DP, Wagner NJ (2009) Microstructure of shear-thickening concentrated suspensions determined by flow-USANS. Rheol Acta 48:897–908

Kang TJ, Kim CY, Hong KH (2012) Rheological behavior of concentrated silica suspension and its application to soft armor. J Appl Polym Sci 124:1534–1541

Komal RP, Sunny RS and Navin RS (2011) Preparation, characterization, and in vitro evaluation of ezetimibe binary solid dispersions with poloxamer 407 and PVP K30. J Pharm Innov 6:107–114

Laun HM, Bung R, Hess S, Loose W, Hess O, Hahn K, Hadicke E, Hingmann R, Schmidt F, Lindner P (1992) Rheological and small angle neutron scattering investigation of shear-induced particle structures of concentrated polymer dispersions submitted to plane Poiseuille and Couette-flow. J Rheol 36:743–787

Lee YS, Wetzel ED, Wagner NJ (2003) The ballistic impact characteristics of Kevlar R woven fabrics impregnated with a colloidal shear thickening fluid. J Mater Sci 38:2825–2833

Liu M, Jiang WQ, Chen Q, Wang S, Mao Y, Gong XL, Leung KCF, Tian J, Wang HJ, Xuan SH (2016) A facile one-step method to synthesize SiO_2@polydopamine core–shell nanospheres for shear thickening fluid. RSC Adv 6:29279

Maranzano BJ, Wagner NJ (2001) The effects of particle size on reversible shear thickening of concentrated colloidal dispersions. J Chem Phys 114:10514–10527

Namekawa K, Kaneko A, Sakai K, Kunikata S, Matsuda M (2011) Longer storage of dialyzers increases elution of poly(N-vinyl-2-pyrrolidone) from polysulfone-group dialysis membranes. J Artif Organs 14:52–57

Newstein MC, Wang H, Balsara NP, Lefebvre AA, Shnidman Y, Watanabe H, Osaki K, Shikata T, Niwa H, Morishima Y (1999) Microstructural changes in a colloidal liquid in the shear thinning and shear thickening regimes. J Chem Phys 111:4827–4838

O'Brien VT, Mackay ME (2000) Stress components and shear thickening of concentrated hard sphere suspensions. Langmuir 16:7931–7938

Parmar KR, Shah SR, Sheth NR (2011) Preparation, characterization, and in vitro evaluation of ezetimibe binary solid dispersions with Poloxamer 407 and PVP K30. J Pharm Innov 6: 107–114

Qin J, Zhang G, Shi X, Tao M (2015) Study of a shear thickening fluid: the dispersions of silica nanoparticles in 1-butyl-3-methylimidazolium tetrafluoroborate. J Nanopart Res 17:333

Seto R, Mari R, Morris JF, Denn MM (2013) Discontinuous shear thickening of frictional hard-sphere suspensions. Phys Rev Lett 111:218301

Sha X, Yu K, Cao H, Qian K (2013) Shear thickening behavior of nanoparticle suspensions with carbon nanofillers. J Nanopart Res 15:1816

Shenoy SS, Wagner NJ (2005) Influence of medium viscosity and adsorbed polymer on the reversible shear thickening transition in concentrated colloidal dispersions. Rheol Acta 44: 360–371

Stöber W, Fink A, Bohn E (1968) Controlled growth of monodisperse silica spheres in the micron size range. J Colloid Interface Sci 26:62–69

Swei J, Talbot JB (2003) Viscosity correlation for aqueous Polyvinylpyrrolidone (PVP) solutions. J Appl Polym Sci 90:1153–1155

Wagner N J, Wetzel E D (2007) US Patent 7, 226, 878

Warren J, Cole M, Offenberger S, Lacy TE, Toghiani H, Burchell M, Pittman CU (2013) Hypervelocity Impact of Honeycomb Core Sandwich Panels Filled with Shear Thickening Fluid. In 28th Technical Conference of the American Society for Composites, State College

Xu YL, Gong XL, Peng C, Sun YQ, Jiang WQ, Zhang Z (2010) Shear thickening fluids based on additives with different concentrations and molecular chain lengths. Chin J Chem Phys 23:342–346

Yang HG, Li CZ, Gu HC, Fang TN (2001) Rheological behavior of titanium dioxide suspensions. J Colloid Interface Sci 236: 96–103

Ye F, Zhu W, Jiang WQ, Wang ZY, Chen Q, Gong XL, Xuan SH (2013) Influence of surfactants on shear-thickening behavior in concentrated polymer dispersions. J Nanopart Res 15:2122

Yu K, Cao H, Qian K, Sha X, Chen Y (2012) Shear-thickening behavior of modified silica nanoparticles in polyethylene glycol. J Nanopart Res 14:747

Zhang XZ, Li WH, Gong XL (2008) The rheology of shear thickening fluid (STF) and the dynamic performance of an STF-filled damper. Smart Mater Struct 17:035027